C. D. Ertley, O. H. W. Siegmund, S. R. Jelinsky, J. Tedesco, M. J. Minot, A. O'Mahony, C. A. Craven, M. Popecki, A. V. Lyashenko, M. R. Foley "Second Generation Large Area Microchannel Plate Flat Panel Phototubes", SPIE Astronomical Telescopes + Instrumentation 26 June - 1 July 2016

Second Generation Large Area Microchannel Plate Flat Panel Phototubes

C. D. Ertley*[a], O. H. W. Siegmund[a], S. R. Jelinsky[a], J. Tedesco[a], M. J. Minot[b], A. O'Mahony[b], C. A. Craven[b], M. Popecki[b], A. V. Lyashenko[b], M. R. Foley[b]

[a]Experimental Astrophysics Group, Space Sciences Laboratory, 7 Gauss Way, University of California, Berkeley, CA 94720

[b]Incom, Inc. 294 Southbridge Road, Charlton, MA 01507

ABSTRACT

Very large (20 cm × 20 cm) flat panel phototubes are being developed which employ novel microchannel plates (MCPs). The MCPs are manufactured using borosilicate microcapillary arrays which are functionalized by the application of resistive and secondary emissive layers using atomic layer deposition (ALD). This allows the operational parameters to be set by tailoring sequential ALD deposition processes. The borosilicate substrates are robust, including the ability to be produced in large formats (20 cm square). ALD MCPs have performance characteristics (gain, pulse amplitude distributions, and imaging) that are equivalent or better than conventional MCPs. They have low intrinsic background (0.045 events cm^{-2} sec^{-1})., high open area ratios (74% for the latest generation of borosilicate substrates), and stable gain during >7 C cm^{-2} charge extraction after preconditioning (vacuum bake and burn-in). The tube assemblies use a pair of 20 cm × 20 cm ALD MCPs comprised of a borosilicate entrance window, a proximity focused bialkali photocathode, and a strip-line readout anode. The second generation design employs an all glass body with a hot indium seal and a transfer photocathode. We have achieved >20% quantum efficiency and good gain uniformity over the 400 cm^2 field of view, spatial resolution of <1 cm and obtained event timing accuracy of close to 100 ps FWHM.

Keywords: Microchannel Plate, Imaging, Photon Counting, Atomic Layer Deposition

1. INTRODUCTION

Large area detectors with spatial resolution of < 1 mm and timing resolution on the order of a few picoseconds are highly desirable for many applications such as the detection of Cherenkov light in neutrino detectors and neutron detectors. Commercially available devices cannot meet these requirements due to size and timing limitations of conventional microchannel plates (MCPs) or of photo multipliers with dynode amplification. We are pursuing the development of a "flat panel" scheme for devices as large as 20 cm × 20 cm utilizing novel MCPs. This effort, undertaken by the Berkeley Space Sciences Laboratory and Incom, Inc., derives from the LAPPD collaboration of universities, Argonne National Laboratory, and commercial companies[1].

The large area flat panel detector concept is similar to conventional sealed tube MCP detectors. The design includes an entrance window (Borofloat-33) with a semitransparent photocathode on the inside surface. A gapped MCP pair detects and amplifies the photoelectron produced by the photocathode. The resulting electron cloud is detected by a strip line anode. Power is supplied to each layer to produce the needed voltage differential for accelerating the electrons. Figure 1 shows and expanded view illustration of the glass body flat panel photodetector concept.

The 400 cm^2 device format presents some unique challenges for hermetic sealing: a large entrance window, a 400 cm^2 semitransparent photocathode with good efficiency and uniformity, 20 cm × 20 cm MCPs, and robust construction to withstand the atmosphere pressure differential. The first generation of flat panel detectors were assembled using a ceramic body design based on conventional sealed tube Kovar/ceramic brazed assemblies[2]. The second generation tubes utilize an all glass lower tile assembly (LTA). The LTA includes a base plate with painted on silver anode strips and HV connections in each corner. A sidewall with a machined indium well that facilitates hot sealing to a Borofloat-33 entrance window is attached to the base with a glass frit seal (Fig. 2). The base is slightly larger than the sidewall in one axis to provide access to the anode strips and HV connections. Like the ceramic body, the MCPs are clamped between ceramic "X's" that accommodate the stress load for an atmosphere pressure differential (Fig. 3). High vacuum inside the

* camden.ertley@ssl.berkeley.edu; phone: 1 (510) 664-4699; fax: 1 (510) 643-9729; www.ssl.berkeley.edu/

tube is maintained after sealing by installing 16 heat activated getters beneath the MCPs. Reasonable sensitivity, a low background event rate, high conductivity and high stability is obtained using a high temperature bialkali photocathode[3].

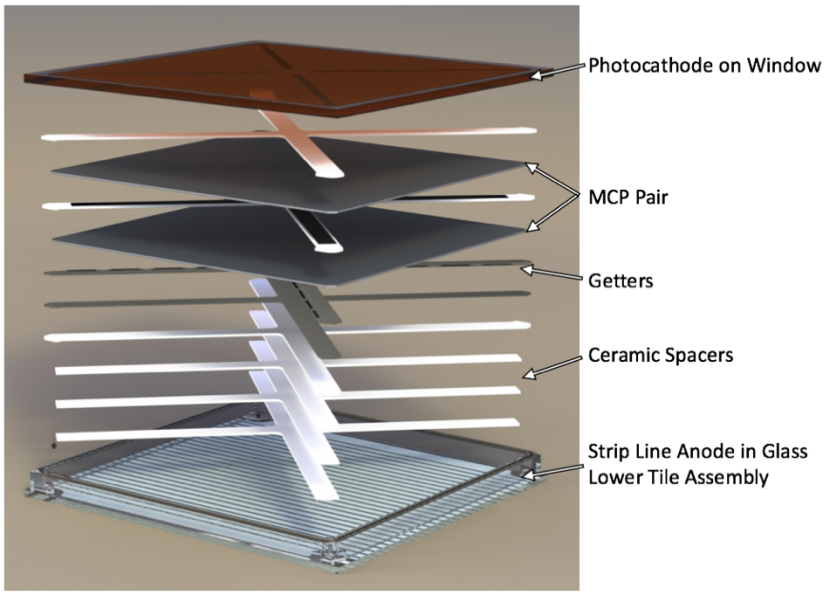

Fig. 1: Depiction of the glass body flat panel microchannel plate detector. Incoming photons pass through an entrance window and are converted to photoelectrons by a semitransparent photocathode. A microchannel plate stack multiplies the photoelectron events and the resulting charge is sensed by a strip-line anode.

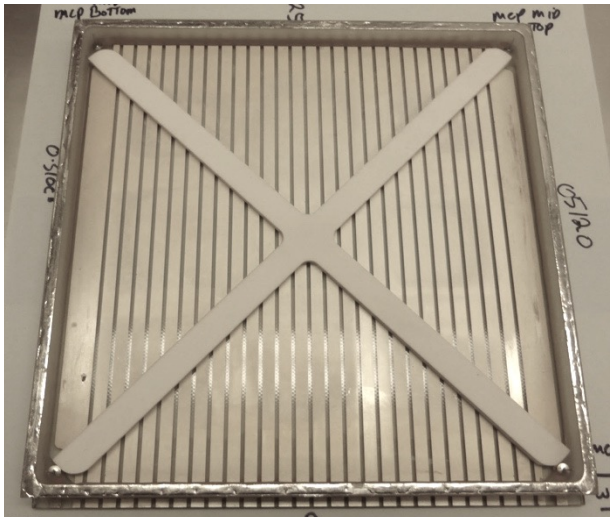

Fig. 2: Lower tile assembly for the 20 cm × 20 cm "flat panel" microchannel plate detector with bottom ceramic spacers. The all glass body has a strip-line anode on the base plate. The base plate extends outside the sidewall in one axes to accommodate readout of the anode and high voltage connections.

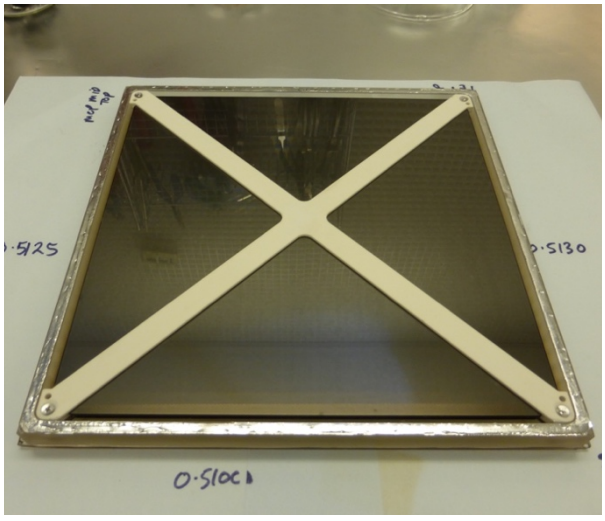

Fig. 3: The 20 cm × 20 cm lower tile assembly shown with the microchannel plates installed. Corner pins secure the stack. The indium well is filled and prepared for the hot seal.

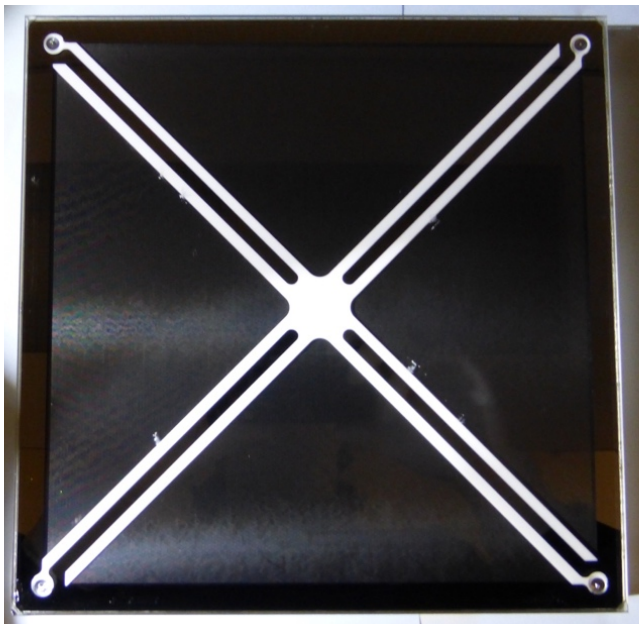

Fig. 4: Completed glass body "flat panel" detector. The top ceramic "X" spacer is clearly visible with metalized fingers. The borosilicate window is bonded to LTA with a hot indium seal. High vacuum is maintained by heat activated getters.

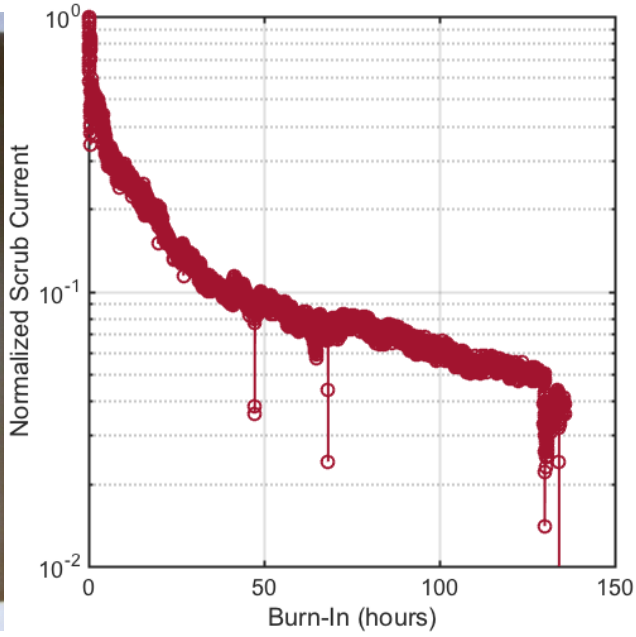

Fig. 5: Preconditioning burn-in. The gain dropped by a factor 10 within 48 hours and leveled off thereafter. This step is essential to stabilizing the MCP gain and minimizing the effects of gas evolution during the life of a sealed tube.

2. 20 CM SEALED TUBE CONSTRUCTION

The MCPs, spacers, and getters shown in Fig. 1 are assembled and installed in the LTA. Pins in each corner of the LTA distribute power to the MCP stack layers and are used to anchor the assembly. Initial testing after assembly is done in the processing chamber to establish the operation of the unit (gain, background, imaging). Once verified, there is a vacuum bake followed by a "burn-in" to stabilize the MCP operation. Photocathode deposition on the window and finally a hot indium window seal completes the tube. This report summarizes results obtained for two glass body tubes that were attempted at SSL during the period from June 2015 through August 2015 (the second completed tube is shown in Fig 4).

In order to remove most of the residual gases and to clean all the internal surfaces in preparation of sealing, the loaded processing tank goes through a high vacuum bake, lasting ~24 hours and peaking at ~350°C. During the bake, a residual gas analyzer was used to monitor the pressures and gas evolution. As the temperatures approached the peak value, water vapor and atmospheric gases increased several orders of magnitude. After peaking in the low 10^{-5} torr range, the pressure slowly decreased to low levels (< 10^{-7} torr). After cooling to room temperature, the pressure in the tank reached the low 10^{-10} torr levels. The bake produced no substantial changes in the operation as seen by the gain, imaging, and background of the detector.

Stabilization of the MCP operation and minimization of the gas emission from the MCPs is accomplished by a charge extraction "burn in" or "scrub" after the bake. Minimizing the effects of gas evolution are essential to the longevity of the device, reducing performance changes, and preventing ion feedback damage [4,5]. The charge extraction during the "burn in" of the glass body flat panel assembly is shown in Fig. 5. The gain dropped by a factor 10 within 48 hours and leveled off thereafter, in accord with earlier observations for this type of MCP[6].

The process for depositing semitransparent Na_2KSb bialkali photocathodes on 20 cm × 20 cm format Borofloat-33 windows was matured using trial depositions[7] and two ceramic flat panel process runs[2]. The properties of this type of photocathode, low background rate, high conductivity, and high temperature tolerance compared with other bialkali photocathode types[3], make it an ideal candidate for the flat panel detector. The flat panel tube processing uses a window

"transfer process" after the photocathode has been deposited followed by a hot indium seal. Shortly after the photocathode deposition, the quantum efficiency was measured in comparison to a standard photodiode. The QE was much lower than expected for this initial glass device process, 0.2% at 356 nm, which has been attributed to contamination on the window surfaces. Even with this very low QE, signals from the photocathode were still present (Fig. 12 & 13).

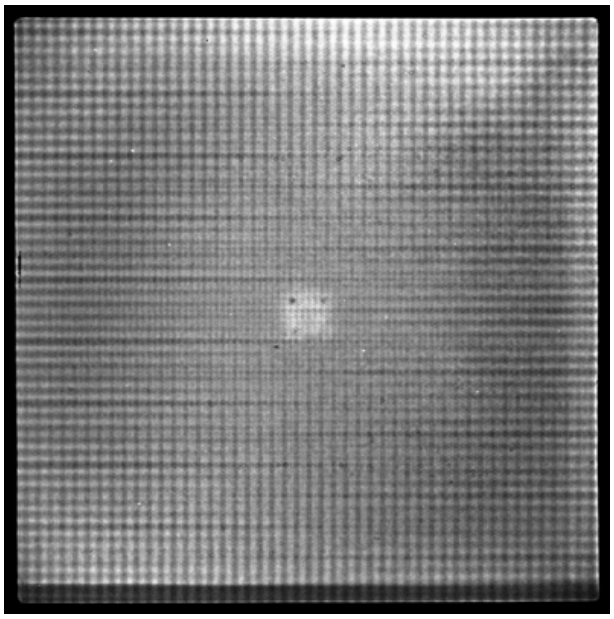

Fig. 6: Flat field image with 185 nm illumination. ALD borosilicate MCP pair, 20 µm pore, 60:1 L/d, 8° bias, 0.7 mm/200 V MCP pair gap/bias, at 1 x 10^7 gain, 1000/850 V bias on the top/bottom MCP.

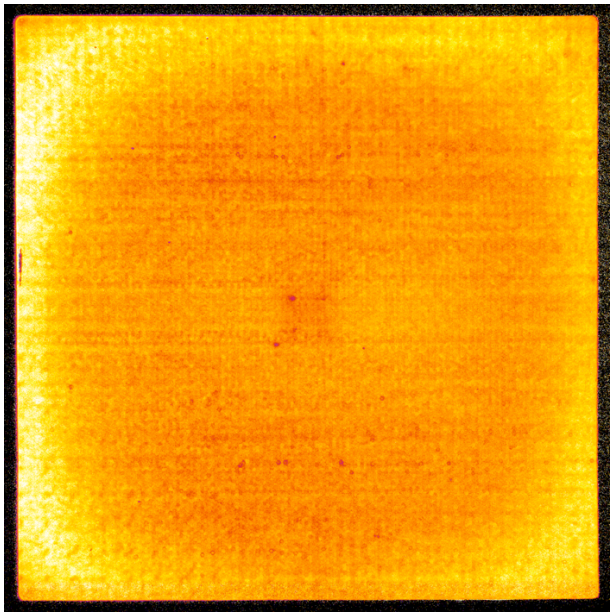

Fig. 7: Flat field "gain" map image using 185 nm illumination. ALD borosilicate MCP pair, 20 µm pore, 60:1 L/d, 8° bias, 0.7 mm/200 V MCP pair gap/bias, at 1 x 10^7 gain, 1000/850 V bias on the top/bottom MCP.

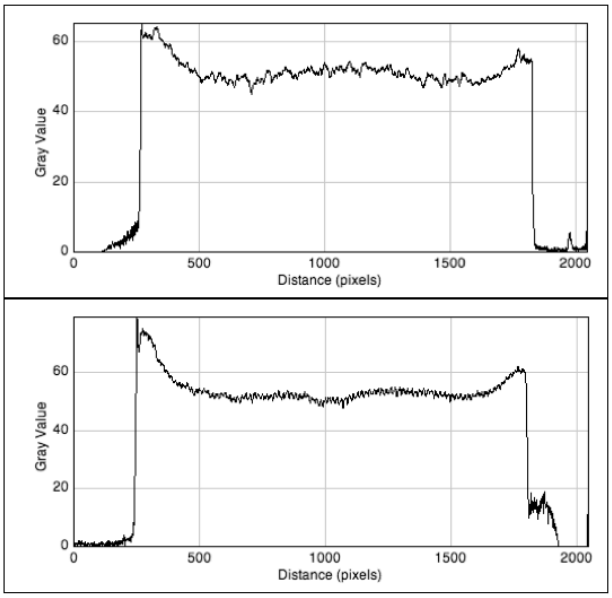

Fig. 8: Gain uniformity histogram of the image shown in Fig. 7. The average gain of 1.0×10^7 varies by ~15%.

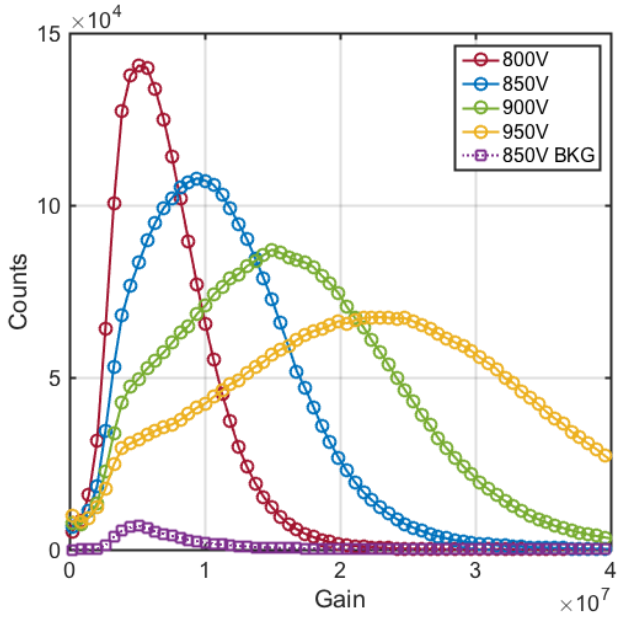

Fig. 9: Pulse amplitude distribution from a borosilicate ALD MCP pair. Both MCPs have 20 µm pore, 60:1 L/d, 8° bias. 0.7 mm/200 V MCP pair gap/bias, Top MCP was set to 1000V and the bottom MCP voltage was varied.

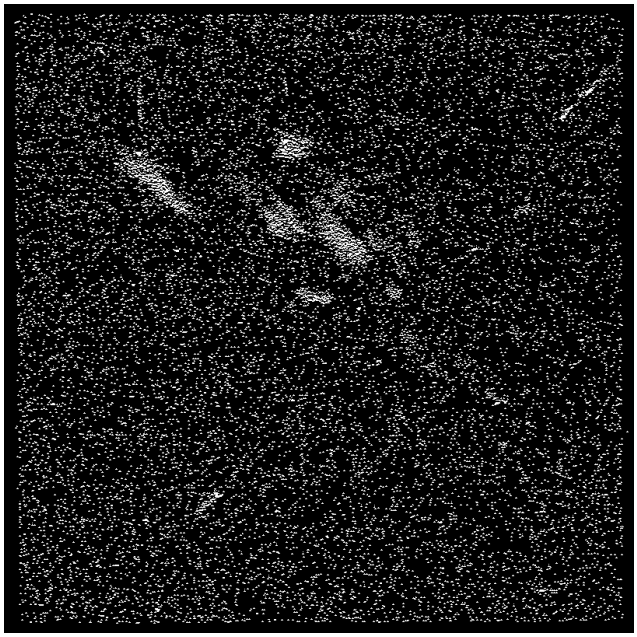

Fig. 10: Background image. 0.36 cts sec^{-1} cm^{-2}. 0.045 cts sec^{-1} cm^{-2} excluding hot spots. ALD borosilicate MCP pair, 20 µm pore, 60:1 L/d, 8° bias, 0.7 mm/200 V MCP pair gap/bias, at 1 x 10^7 gain, 1000/850 V bias on the top/bottom MCP.

3. IMAGING AND GAIN CHARACTERISTICS

Large area MCPs are constructed using borosilicate microcapillary arrays functionalized with atomic layer deposition (ALD). Unlike conventional MCP construction[8], which uses H_2 reduction to change lead glass substrate into a secondary emitting surface, the functionalization is decoupled from the borosilicate substrate. The ALD MCP micro-capillary substrate is constructed from borosilicate tubes by drawing and fusing an array that is made to function as an MCP by deposition of resistive and secondary emissive layers using ALD[9, 10]. Sequential ALD steps allow the operational parameters, such as resistance, to be tailored to the specific application. ALD MCPs can suffer from some of the same issues common to all MCPs, including cleanliness, minimization of pore crushing at the multifiber boundaries and establishing uniform pore sizes over the entire substrate.

The large area flat panel detector project is made possible due to the robust borosilicate substrates used in ALD MCP construction. They can be produced in the 20 cm × 20 cm format needed for the project with pore sizes in the 40 µm to 10 µm range. The standard MCP used in the flat panel detector has 20 µm pores, 60:1 pore L/d ratio, and 8° pore bias angle. There has been much improvement in the quality of the substrates since the first generation[11], which suffered from significant pore size non-uniformity and multifiber boundary distortions that produced significant image modulation[12]. The latest generation of substrates manufactured by Incom, Inc., have improved structures as seen by optical inspection and operational data and can be made with open area ratios up to values of 74%. The resistive and secondary emissive ALD layers have been shown to match and in some respects exceed conventional MCP performance characteristics[13]. The ALD resistive layer has been optimized[9] and coatings of Al_2O_3 and MgO have been used as the secondary emissive layer.

Evaluations of the ALD MCPs before installation in a sealed tube detector are performed using a photon counting imaging detector that employs a pair of MCPs and a cross delay line readout anode[14]. The MCPs are spaced 0.7 mm apart with a 200 V bias applied over the gap and have a ~10 mm MCP output to anode gap. The anode is a cross delay line readout with a 20 cm x 20 cm active area, a 4 mm period, and ~100 ns end to end delay time. This anode design supports equal charge sharing between the upper and lower orthogonal serpentine conductors permitting high overall event rate encoding and modest spatial resolution (~100 µm FWHM)[14].

During the MCP evaluation process, a suite of measurements is used to determine candidate MCPs for processing in a flat panel tube detector. Analysis of flat field images taken with 185 nm illumination show the overall uniformity of response (Fig. 6). Along with the flat field image, a gain map image indicates the uniformity of the MCP gain. Gain uniformity is better than 15% over most of the field of view for the MCPs used in the latest tube sealing trials (Fig 7 & 8). Dominant features in the image and gain map are the hexagonal multi-fiber boundaries and the structure of the anode. The small square in the center of Fig. 6 is due to the ALD processing and has been corrected in later MCP generations. Another important characteristic of the MCPs is the gain as a function of applied voltage and the pulse amplitude distribution (Fig. 9). The pulse amplitude show well peaked distributions at gains above 5×10^6 for 20 μm pore, 60/1 L/d, 8° bias angles, using 20 cm × 20 cm MCP pairs (Fig 9).

One major advantage of using borosilicate substrates is the lower alkali metal content in the glass compared to conventional lead glass MCPs. The alkali (K, Rb) beta decay dominates the background rate in conventional MCPs[15] causing higher rates than borosilicate glass MCPs. The background has a uniform spatial distribution (Fig. 10) with an observed rate of 0.045 events sec^{-1} cm^{-2} excluding hot spots. These results are comparable to previous tests of 20 cm × 20 cm MCP pairs[11]. However, the background in the flat panel detector is dominated by the photocathode background (Fig. 14).

Evaluation of the glass body detector happens at several stages in the assembly process. The image resolution is poor due to the speed of the anode signals and the timing resolution of our lab. electronics, but provides essential feedback during and after the tube assembly. The strip line anode was read out as a continuous delay line by connecting the strip ends together at alternating sides in a serpentine fashion. The two ends were connected to our existing amplifier / time to digital encoding electronics. A single channel was used to create a two dimensional position encoding and timing for each individual event. Following the tube processing and sealing, the flat panel detector was evaluated in two modes, one using 100 V MCP to anode gap bias and 100 V cathode to MCP gap bias, and the other by shorting the MCP input and cathode so they were at the same potential. The first mode, "cathode on", permits the full flat panel device operation to be evaluated, while the other, "cathode off", provides information on the performance of the MCP pair.

The first glass body flat panel detector in the "cathode off" mode produced flat field and gain map images using 256 nm illumination at a ~10 kHz rate. The gain map image (Fig. 11 & 12), shows the gain is relatively uniform after sealing the tube, with fluctuations on the order of 25% across both axes. These fluctuations are similar to previous trials with a ceramic body flat panel detector[2].

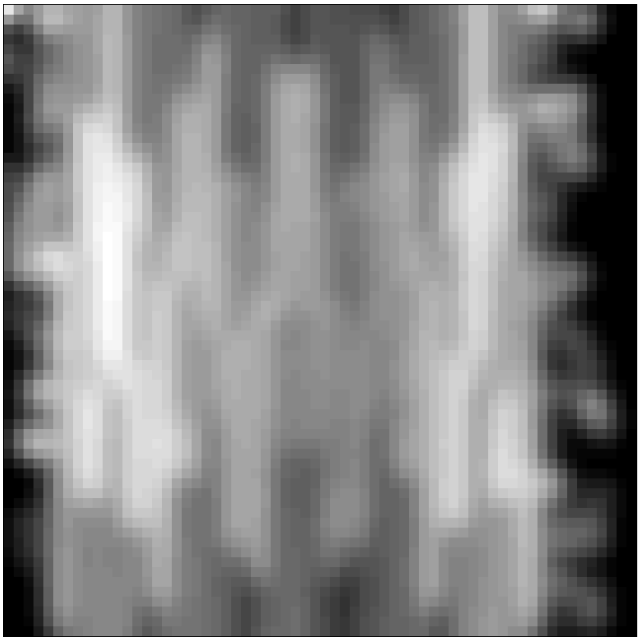

Fig. 11: Flat field "gain map" using 185 nm illumination of the assembled glass body flat panel tube, white is high gain.

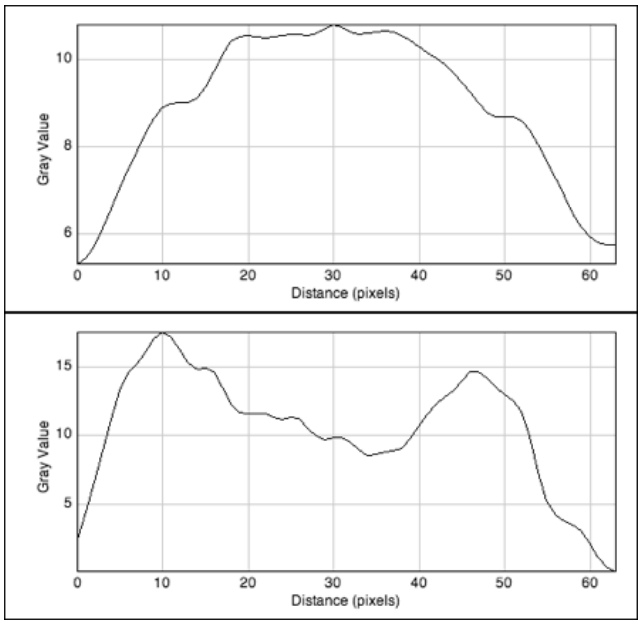

Fig. 12: Histogram of the gain map shown in Fig. 11.

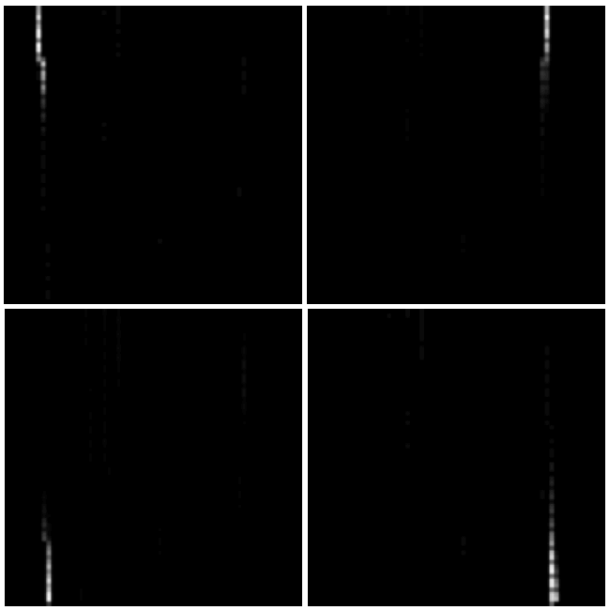

Fig. 13: 405 nm Pilas laser spot imaging from the completed flat panel tube. 4 images, each with a different laser spot position, are shown. Resolution is much better in the X-axes, ~3 mm FWHM, than the Y-axes, ~16 mm FWHM.

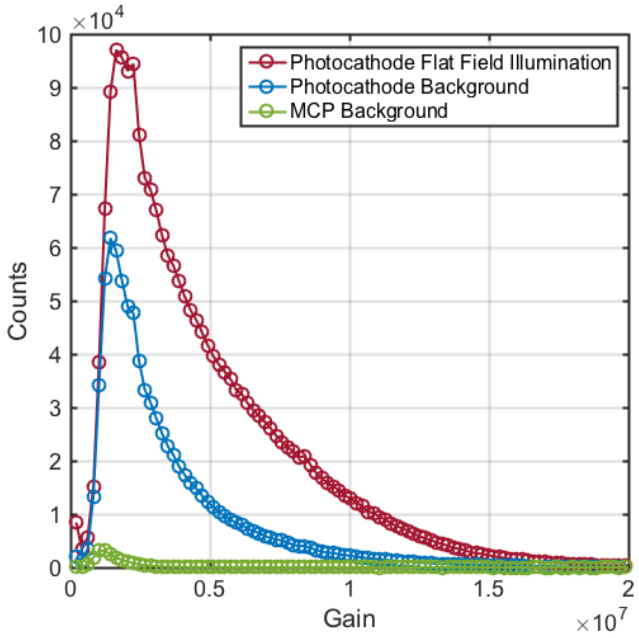

Fig. 14: Pulse height amplitude distributions for the completed flat panel detector with the photocathode unbiased (MCP signal only) and with the cathode biased at 100 V. MCP background ~1 events cm^{-2} s^{-1}. Cathode background ~54 events cm^{-2} s^{-1}. MCP bias of ~1000/850 V on the top/bottom MCP.

Even with the reduced resolution in this configuration, imaging is possible. In the "cathode on" mode, a 405 nm Pilas laser was used to take several images were with different laser spot locations (Fig. 13). The image resolution is much better in the X-axis, ~ 3 mm FWHM, than it is in the Y-axis, ~16 mm FWHM, because the X-position comes from the strip number which collected the charge cloud while the Y-position comes from the timing of the signals. The quantum efficiency (QE) of the photocathode was measured after deposition while the tube was still hot. The low QE, on the order of 0.2% at 356 nm, may be attributed to contamination on the window. The earlier trial runs showed QEs of 25% at 356 nm were achievable and repeatable[2].

4. TIMING CHARACTERISTICS

The timing resolution of the glass body flat panel detector was examined by attaching a fast amplifier (VT100, ~100 ns risetime) to the anode. The signals from the fully assembled and processed detector using a Pilas laser (~45 ps timing jitter) with ~10 photoelectrons produced per pulse are shown in Figure 15. The connections to the detector anode, while in the processing tank, have not been optimized for impedance matching. The temporary connections and the amplifier performance dominate the ~4 ns pulse width. The time interval between the laser trigger and the detector signal are measured by a time to digital converter. The timing resolution is dominated by the time to digital converter electronics. The electronics, with a resolution of ~70 ps FWHM, and the laser trigger jitter, with a resolution of ~45 ps, result in a limiting timing resolution of about 100 ps.

The transit time jitter is highly dependent on the source and the bias voltages in the detector. The timing resolution was measured for different source intensities (Fig. 16), as well as, MCP to anode gap (Fig. 17) and cathode to MCP gap (Fig. 18) bias voltages. The source intensity was varied while keeping the gap bias voltages the same. Very large signals resulted in much better timing resolution, 48 ps FWHM at 1000 pe- per pulse (Fig 16). The dependence of the timing resolution on the rear field accelerating voltage, MCP to anode, shows an improvement up ~150 V. The timing accuracy of the glass body detector is slightly worse than that measured with the ceramic body detector[2], ~175 ps FWHM compared to ~120 ps FWHM under comparable conditions. This is due to the larger MCP to anode gap distance in the glass body detector, which allows for more lateral drift of the electrons exiting the bottom of the MCP after

multiplication and results in wider pulse widths. The timing resolution improved by a large amount while varying the photocathode to MCP proximity gap accelerating voltage (Fig. 18), but resulted in similar timing resolutions to the ceramic tube at higher voltages[2].

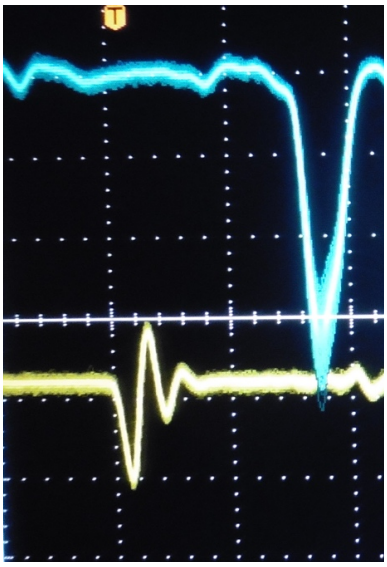

Fig. 15: Laser pulse signals (~10 photoelectrons per pulse) from a 405 nm Pilas laser with ~45 ps timing jitter. Flat panel detector gain of ~1 x 10^7 with fast signals from the anode amplified by an Ortec VT100 preamp giving pulse widths of ~2.5 ns. Both traces are 200 mV per division and 10 ns per division.

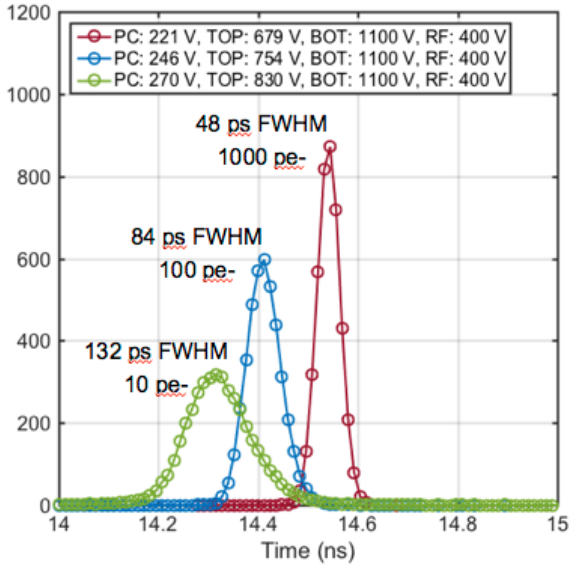

Fig. 16: Laser pulse signal timing jitter from a 405 nm Pilas laser (~45 ps timing jitter) using 3 different neutral density filters. Flat panel detector gains of ~1 x 10^7, cathode gap bias ~250 V, anode gap bias 400 V.

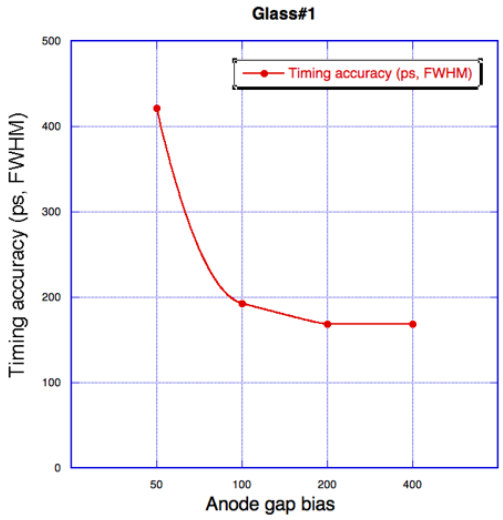

Fig. 17: Laser pulse signal timing jitter (~10 photoelectrons per pulse) from a 405 nm Pilas laser (~45 ps timing jitter). Flat panel detector gain ~1 x 10^7, photocathode gap bias 200 V. Increasing the anode gap (7 mm) bias shows modest timing improvements.

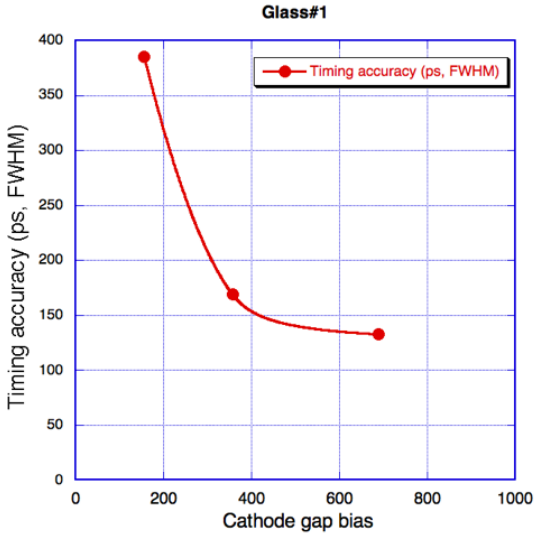

Fig. 18: Laser pulse signal timing jitter (~10 photoelectrons per pulse) from a 405 nm Pilas laser (~45 ps timing jitter) as a function of the cathode gap (1.5 mm) bias. Flat panel detector gain ~1 x 10^7, anode bias 100 V.

5. CONCLUSIONS

Two glass body flat panel detectors were attempted, but both leaked and returned to atmospheric pressures shortly after being removed from the processing tank. Testing while in the processing tank provided useful performance metrics on the glass body package for comparison with the ceramic body package. ALD MCPs have been shown to have many advantages over conventional MCP, including low outgassing, short burn-in times, and stable performance. The performance of the assembled glass body tube was not as good as the ceramic package tubes, due to mismatched electronics, a larger MCP to anode gap, and contamination of the photocathode. Even with these issues, the tube was capable of imaging a 405 nm Pilas laser, had relatively low background rates (~54 events s^{-1} cm^{-2} from the photocathode), and good timing resolution (48 ps FWHM with ~1000 photoelectrons and 5×10^6 gain). The timing and imaging resolutions were dominated by the limitations of the electronics and will be greatly improved by the final electronics implementations.

ACKNOWLEDGEMENTS

We wish to thank the members of the team at Incom, Inc., Dr. J. Elam, Dr. R. Wagner and Dr. A. Mane at Argonne National Laboratory, and Prof. H. Frisch at University of Chicago for their contributions to this work. This work was supported by RCUH contract Z10086536.

REFERENCES

[1] "Large-Area picosecond Photo-Detectors Project," http://psec.uchicago.edu (28 May 2016).

[2] Siegmund, O. S. W., Ertley, C. D., Jelinsky, S. R., McPhate, J. B., Tedesco, J., Minot, M. J., O'Mahony, A., Craven, C. A., "Very Large Area 20cm x 20cm Flat Panel Phototubes Using ALD Microchannel Plates," IEEE Trans. Nucl. Sci. (in press)

[3] Lyashenko, A. V., Breskin, A., Chechik, R., Veloso, J. F. C. A., Santos, Dos, J. M. F., Amaro, F. D., "Development of high-gain gaseous photomultipliers for the visible spectral range," J Instrum **4**, (2009).

[4] Uhlig, F., Britting, A., Eyrich, W., Lehmann, A., Schwarz, C., Schwiening, J., "Performance studies of microchannel plate PMTs," Nucl. Instr. Meth. Phys. Res. A **695**, 68–70 (2012).

[5] Siegmund, O. H. W., "Preconditioning Of Microchannel Plate Stacks," Proc. SPIE **1072**, (1989).

[6] Ertley, C. D., Siegmund, O. S. W., Hull, J. S., Tremsin, A., O'Mahony, A., Craven, C. A., Minot, M. J., "High Dynamic Range Photon Counting Imagers Using Nano-Engineered Microchannel Plates," IEEE Trans. Nucl. Sci. (in press)

[7] Siegmund, O. H. W., Vallerga, J., Tremsin, A., McPhate, J., Frisch, H., Elam, J., Mane, A., Wagner, R., Varner, G., "Large Area and High Efficiency Photon Counting Imaging Detectors with High Time and Spatial Resolution for Night Time Sensing and Astronomy," Advanced Maui Optical and Space Surveillance Technologies Conference, 92 (2012).

[8] Lampton, M., "The Microchannel Image Intensifier," Scientific American **245**(5), 62–71 (1981).

[9] Mane, A. U., Peng, Q., Wetstein, M. J., Wagner, R. G., Frisch, H. J., Siegmund, O. H. W., Minot, M. J., Adams, B. W., Chollet, M. C., et al., "A novel atomic layer deposition method to fabricate economical and robust large area microchannel plates," Proc. SPIE **80312**, (2011)

[10] Ritala, M., Leskelä, M., "Atomic layer epitaxy - a valuable tool for nanotechnology?," Nanotechnology **10**, 19–24, IOP Publishing (1999).

[11] Ertley, C., Siegmund, O. H. W., Schwarz, J., Mane, A. U., Minot, M. J., O'Mahony, A., Craven, C. A., Popecki, M., "Characterization of borosilicate microchannel plates functionalized by atomic layer deposition," Proc. SPIE **9601**, (2015).

[12] Siegmund, O. H. W., McPhate, J. B., Vallerga, J., Tremsin, A., Jelinsky, S. R., Frisch, H. J., "Novel large format sealed tube microchannel plate detectors for Cherenkov timing and imaging," Nucl. Instr. Meth. Phys. Res. A **639**(1), 165–168 (2011).

[13] Siegmund, O. H. W., Ertley, C., Vallerga, J., "High Speed Large Format Photon Counting Microchannel Plate Imaging Sensors," Proceedings of the Advanced Maui Optical and Space Surveillance Technologies Conference, held in Wailea, Maui, Hawaii, September 15-18, 2014, Ed.: S. Ryan, The Maui Economic

Development Board, id.94 **-1**, 94 (2015).
[14] Siegmund, O. H. W., McPhate, J., Frisch, H., Elam, J., Mane, A., Wagner, R., Varner, G., "Large Area Flat Panel Imaging Detectors for Astronomy and Night Time Sensing," presented at Proceedings of the Advanced Maui Optical and Space Surveillance Technologies Conference, September 2013.
[15] Siegmund, O. H. W., "Methods of vacuum ultraviolet physics," [Vacuum Ultraviolet Spectroscopy], D. L. Ederer and J. A. R. Samson, Eds., Academic Press (1998).